SRR-Loaded SIW-Backed Cavity Sinuous Spiral Antenna for 60 GHz Applications

Boubaker Kerboub
LHS Laboratory, Electronics Department, University of Frères Mentouri - Constantine 1, Constantine, Algeria
boubaker.kerboub@doc.umc.edu.dz (corresponding author)

Siham Benkouda
LHS Laboratory, Electronics Department, University of Frères Mentouri - Constantine 1, Constantine, Algeria
benkouda.siham@umc.edu.dz

Djamel Khezzar
Laboratory of Signal and Systems Analysis, Department of Electronics, Mohamed Boudiaf University, M'sila, Algeria
djamel.khezzar@univ-msila.dz

Salim Ghoggali
Higher National School of Renewable Energy, Environment, and Sustainable Development (HNS-RE2SD), Algeria
salim.ghoggali@hns-re2sd.dzm

Tarek Fortaki
LEA Laboratory, Electronics Department, University of Batna 2, Batna, Algeria
t.fortaki@univ-batna2.dz

Received: 24 March 2025 | Revised: 18 April 2025 | Accepted: 1 May 2025

Licensed under a CC-BY 4.0 license | Copyright (c) by the authors | *DOI: https://doi.org/10.48084/etasr.10972*

ABSTRACT

This paper presents a compact sinuous spiral antenna integrated with a soft surface structure, featuring a square ring placed directly above a Substrate Integrated Waveguide (SIW)-backed cavity, designed for 60 GHz frequency applications. The antenna design achieves a compact size while delivering a wide bandwidth, approximately 16 GHz, covering the entire 60 GHz unlicensed band. It achieves a peak gain of 14 dBi at 70 GHz and a gain above 8 dBi for the rest of the operating band, making it an excellent choice for Millimeter-Wave (mm-Wave) communication systems. Combining the soft surface structure and SIW cavity enhances radiation efficiency and performance. The proposed design effectively suppresses surface wave propagation, minimizing losses and improving radiation characteristics. The simulation results demonstrate the antenna's effectiveness for next-generation wireless communication systems, including 5G and high-speed networks.

Keywords-sinuous spiral antenna; SIW-backed cavity; Split Ring Resonator (SRR); 60 GHz; mm-wave

I. INTRODUCTION

The rapid growth of connected devices and the increasing demand for high data rates—fueled by applications, such as short-range wireless communication, high-definition video streaming, and high-speed internet—have led to the widespread adoption of advanced communication systems [1-3]. To meet these demands, the 60 GHz unlicensed frequency band, part of the mm-Wave spectrum, has emerged as a promising solution [4]. This band exhibits unique propagation characteristics, including significant radio wave absorption due to the resonance of oxygen molecules, rain, and severe path loss [5, 6]. These properties make it especially well-suited for indoor use and provide strong isolation between neighboring cells [7, 8]. The broad bandwidth available in this range supports ultra-high-speed wireless transmission [9]. Moreover, the small antenna size at these frequencies allows for easy integration

with other circuits, resulting in a compact and efficient design, ideal for applications where space and performance are critical [10]. Patch antennas are commonly used in such systems due to their low profile, ease of fabrication, and compatibility with various wireless technologies [11]. However, at higher frequencies, they face challenges, such as limited bandwidth, low gain (typically between 8 dB – 9 dB), and poor Circular Polarization (CP) performance [12]. These limitations are particularly significant at mm-Wave frequencies, where atmospheric attenuation can greatly reduce signal strength and system reliability [8]. While techniques, like ground plane modification and loop feeding, can improve bandwidth, they provide only modest gain enhancements [13]. Superconducting patches offer improvements in both bandwidth and gain, but they come with drawbacks, including the need for cryogenic cooling, the use of specialized materials, and complex integration processes [14, 15].

Conversely, classical sinusoidal spiral antennas are known for their wide bandwidth and the advantage of CP, which effectively reduces multipath interference. Despite these benefits, they are also unsuitable for mm-wave configurations due to their large size and non-planar design. These antennas require a balanced feed to achieve high input impedance, making the fabrication process costly and challenging. To preserve the broadband nature of spiral antennas, some cost-effective and simple alternative feeding techniques have been explored in the literature to eliminate the need for conventional and complex balun structures. These techniques combine the benefits of SIW-backed cavities with spiral antennas. Authors in [1] proposed a spiral CP antenna with a substrate integrated cavity to enhance radiation performance. In [16, 17], instead of a conventional lossy and complicated feed network, a wideband and compact CP spiral antenna array was fed using the PGW SR structure, achieving a high-performance circularly polarized antenna array in the mm-Wave spectrum. In this paper, a four-arm sinusoidal spiral antenna surrounded by soft surface is fed through an aperture on the top face of the SIW-backed cavity. The designed antenna demonstrates good performance, a wide operational bandwidth, and high gain.

II. ANTENNA DESIGN

The design process begins with the construction of the SIW-backed cavity, using Rogers RT/Duroid 5880 as the substrate, which has a dielectric permittivity of $\epsilon r = 2.2$ and a loss tangent of $\tan\delta = 0.0009$. The substrate thickness is 0.787 mm, approximately corresponding to a quarter-wavelength in the dielectric, The SIW cavity structure consists of metallized vias forming the sidewalls, which are integrated into the grounded substrate. A slot is introduced on the upper face of the SIW cavity, acting as an efficient aperture for electromagnetic wave radiation, as depicted Figure 1. The cavity dimensions are 4.6 mm × 4.6 mm. This aperture configuration results in a gain of about 7 dB, and a bandwidth of approximately 7 GHz, ranging from 55 GHz to 62 GHz, as shown in Figure 2.

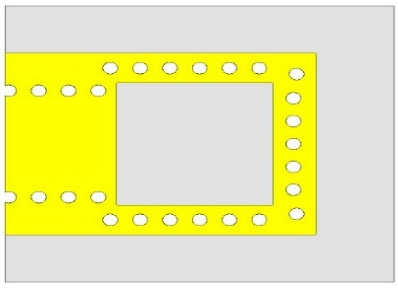

Fig. 1. Primary SIW-backed cavity design.

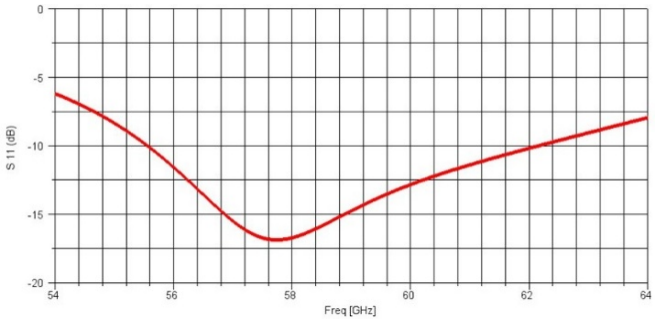

Fig. 2. Obtained return loss of the preliminary antenna.

To achieve a broader bandwidth and higher gain, it is proposed to enhance the aperture either by improving the uniformity of the field distribution or by increasing the physical size of the aperture. In this work, a near-uniform field distribution is approximately achieved. To further improve performance, the aperture size is increased by extending the cavity structure in both length and width. This expansion maintains a low-profile, and a planar configuration with a height of $\lambda g/4$, where λg is the guided wavelength, while preserving the uniformity and strength of the electric field across the aperture. The resulting cavity dimensions are 7.9 mm × 7.9 mm × 0.787 mm. Figure 3 portrays the optimized antenna structure, and its exact dimensions are listed in Table I. Figure 4 presents the return loss of the optimized design, demonstrating an 11.5 GHz bandwidth—from 56.8 GHz to 68.3 GHz—which fully covers the unlicensed 60 GHz band. This marks a notable improvement over the initial design, which exhibited a bandwidth of approximately 7 GHz (from 55 GHz to 62 GHz).

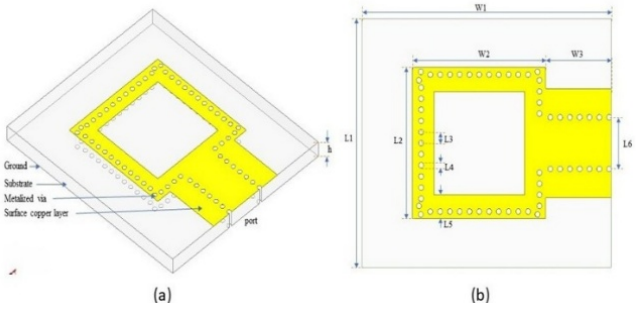

Fig. 3. Optimized SIW-backed cavity design: (a) top view, (b) perspective view.

TABLE I. OPTIMIZED DESIGN PARAMETERS

Parameter	Value mm
L1	13
L2	7.9
L3	0.58
L4	0.15
L5	1.5
L6	2.52
W1	14.77
W2	7.9
W3	3.87
h	0.787

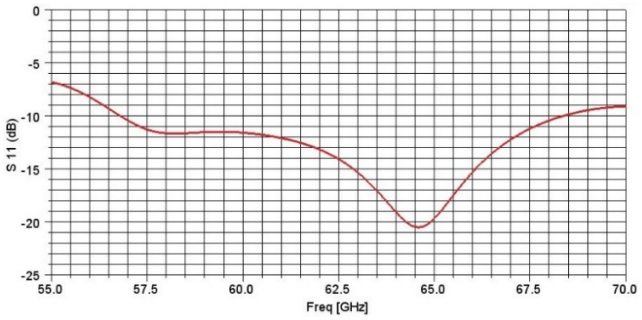

Fig. 4. Obtained return loss of the optimized antenna.

To further enhance performance, a sinuous spiral antenna, surrounded by a soft surface structure consisting of a square ring stacked directly above the cavity, is integrated into the design, as displayed in Figure 5. The sinuous spiral antenna was designed and optimized using the parametric spiral drawing function in HFSS. The geometry follows a frequency-independent spiral formulation defined by the polar coordinates:

$$\varphi = (-1)^P \alpha_P sin\left[\frac{180 \ln\left(\frac{r}{R_p}\right)}{\ln(\ _p)}\right] \quad (1a)$$

and:

$$R_{P+1} \le r \le R_P \quad (1b)$$

$$R_P = \ _{p-1}R_{P-1} \quad (2)$$

where φ and r represent the polar coordinates, P is the cell number, α_P is the angular width that controls how wide each spiral cell spreads in the angular direction around the center, and $_p$ denotes the growth rate governing the radial spacing between arms.

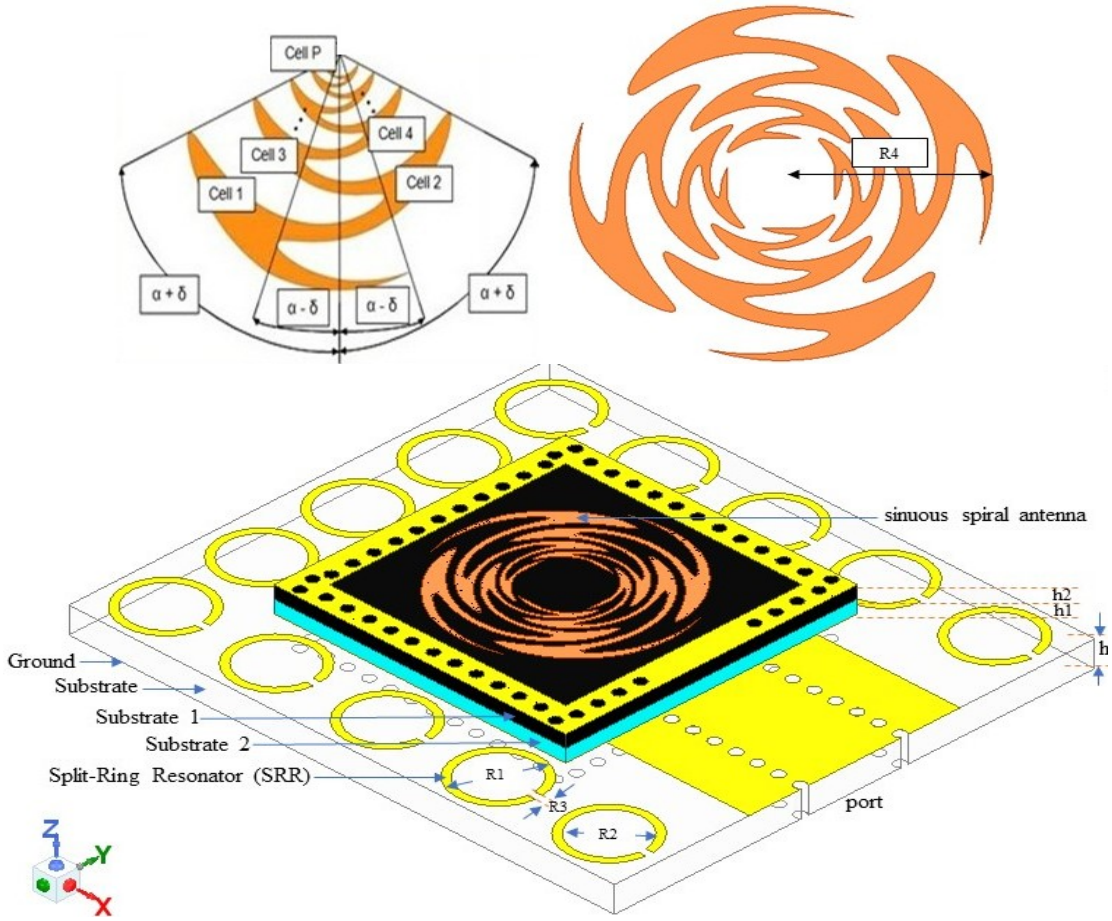

Fig. 5. Geometry of the proposed antenna: (a) sinuous spiral antenna, (b) perspective view of the final design.

The spiral antenna consists of four symmetric arms, with each arm being composed of four cells. These cells form the fundamental building blocks of the sinuous structure, and each plays a role in supporting radiation across a distinct portion of the frequency spectrum. The combination of multiple arms and cells enables the antenna to achieve wideband performance, as the structure maintains effective impedance matching and stable radiation characteristics over a broad frequency range. This geometry is particularly advantageous for mm-Wave applications requiring both high gain and broad bandwidth. The spiral antenna is fed through a coupling aperture etched into the top metal layer of the cavity. This feeding configuration offers several advantages, as highlighted in [18]. The soft surface consists of two dielectric layers: the upper layer has a lower dielectric permittivity, εr = 2.2, while the middle layer has a higher dielectric permittivity, equal to 10. The low-permittivity upper layer facilitates efficient radiation by reducing surface waves, while the high-permittivity middle layer enables strong electromagnetic coupling from the SIW-backed cavity to the spiral antenna. This dielectric stack helps suppress surface wave propagation and backside radiation, enhancing gain, bandwidth, and radiation efficiency.

The metallized vias of the cavity act as sidewalls for the soft surface, creating a short-circuiting effect between the soft surface and the cavity. This configuration suppresses outward propagating surface waves and reduces backside radiation, improving the overall performance of the antenna system. As the cavity walls cannot perfectly confine the energy, the antenna structure was further enhanced by surrounding it with a split-ring resonator. This resonator interacts with the leaked energy from the cavity, resulting in higher gain by effectively trapping and redistributing the energy. A comprehensive parametric sweep was conducted to identify the optimal dimensions for all spiral antenna parameters, including the number of cells, growth rate, angular width, soft surface height, and aperture size. This optimization aimed to mitigate spurious resonances and minimize the excitation of unwanted modes, ensuring stable single-mode operation and enhancing the spectral purity of the antenna. This parametric analysis is crucial as it helps balance the trade-offs between dimensions and various performance metrics, such as gain, bandwidth, and impedance matching. The finalized optimized parameters resulting from this analysis are summarized in Table II.

TABLE I. DESIGN PARAMETERS OF THE FINAL DESIGN ANTENNA

Parameter	Value
R1	1.1 mm
R2	0.9 mm
R3	0.2 mm
h 1	0.64 mm
h 2	0.64 mm
R4	2.82 mm
c	1.3 mm
α	44º
φ	20º

III. RESULTS AND DISCUSSION

This section presents a detailed examination and discussion of the numerical results for the proposed antenna, as shown in Figure 6. The simulated return loss results demonstrate excellent impedance matching over a broad frequency range from 54.4 GHz to 70.6 GHz, yielding a total bandwidth of 16.2 GHz. The minimum return loss of -40 dB occurs at 60 GHz, indicating highly efficient power transfer and minimal signal reflection at this frequency. This deep resonance suggests optimal performance of the antenna at 60 GHz, making it well-suited for mm-Wave applications. The wide operational bandwidth further supports stable impedance matching, reduces transmission losses, and enhances overall system efficiency, highlighting the effectiveness of the proposed design.

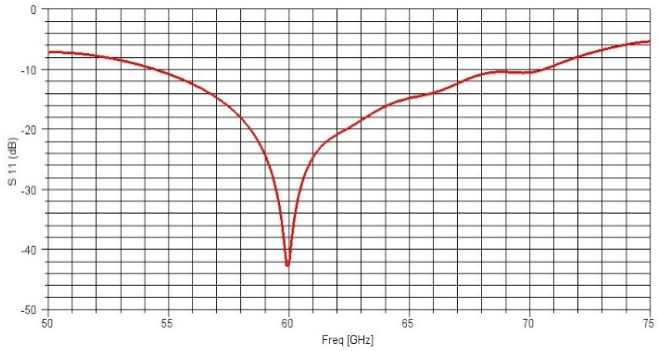

Fig. 6. Obtained return loss of the final design antenna.

Figure 7 illustrates the 3D radiation pattern of the proposed antenna at 60 GHz. The pattern reveals a highly focused main lobe with peak radiation aligned along the Z-axis, indicating strong directional performance. This focused radiation is beneficial for applications, such as point-to-point communication links, where precise targeting is essential. Moreover, the pattern exhibits minimal side lobes, reducing unwanted radiation and interference, which contributes to the overall efficiency and performance of the antenna.

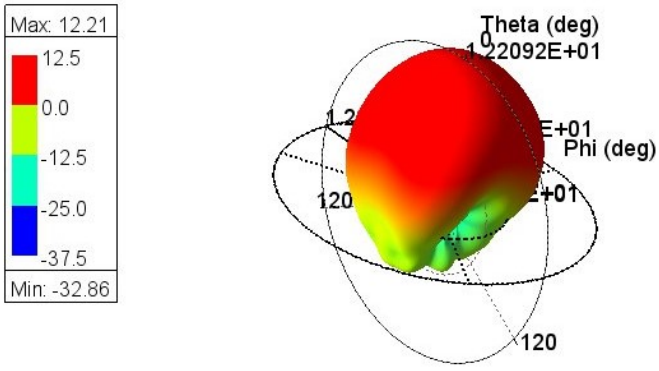

Fig. 7. 3D radiation pattern at 60 GHz.

Figure 8 presents the antenna's gain patterns in both the E-plane and H-plane at frequencies of 55 GHz, 60 GHz, 65 GHz, and 70 GHz. The radiation patterns in both planes are symmetrical, with the main beam and peak gain directed along

the broad side. The measured gain values are 10.8 dB at 55 GHz, 11.5 dB at 60 GHz, 12 dB at 65 GHz, and 14 dB at 70 GHz. These results demonstrate improved antenna efficiency at higher frequencies, reflecting an enhanced ability to focus energy more effectively, which leads to stronger and more reliable signal transmission. Moreover, the antenna consistently maintains low side lobe levels across all frequencies, which is essential for minimizing interference and ensuring clear communication.

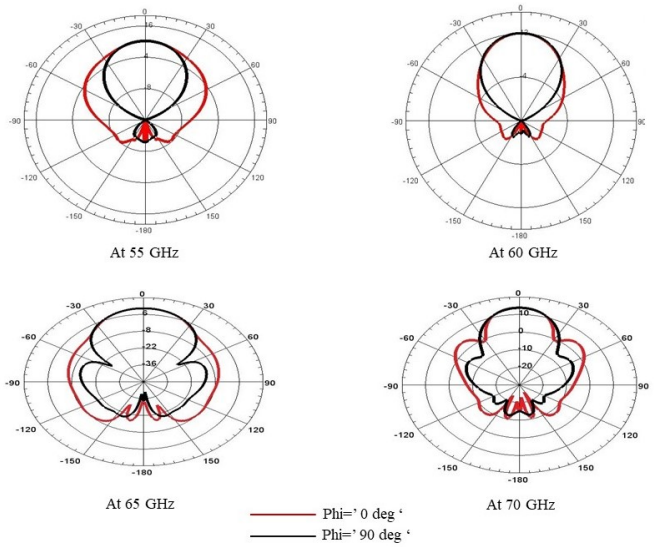

Fig. 8. Radiation patterns in dBi of the antenna at different frequencies within the operating bandwidth.

IV. CONCLUSIONS

This study presents the design and optimization of a high-performance Substrate Integrated Waveguide (SIW)-backed cavity antenna, incorporating a sinuous spiral radiator and a soft surface structure. The initial design featured an SIW cavity with a slot aperture, achieving a 7 dB gain and a 7 GHz bandwidth (55 GHz–62 GHz). To enhance performance, the cavity dimensions were expanded to 7.9 mm × 7.9 mm, increasing the bandwidth to 11.5 GHz (56.8 GHz–68.3 GHz). Further improvements were achieved by integrating a sinuous spiral antenna and a surrounding soft surface structure, which suppressed surface wave propagation and reduced backside radiation. Additionally, the inclusion of a split-ring resonator improved electromagnetic field confinement, boosting the peak gain to 14 dB. The results confirm the antenna's suitability for Millimeter-Wave (mm-Wave) applications, especially in next-generation wireless communication and radar systems. However, some limitations remain. The overall size of the antenna may hinder integration into compact or space-constrained systems. Although a wide bandwidth is achieved, additional enhancement may be required for more demanding applications. Moreover, the use of isotropic substrate materials could limit performance at higher frequencies. Future research should focus on reducing antenna size, exploring advanced bandwidth extension techniques, and investigating anisotropic substrates to further optimize electromagnetic performance [19].

REFERENCES

[1] J. Zhu, S. Liao, S. Li, and Q. Xue, "60 GHz Wideband High-Gain Circularly Polarized Antenna Array With Substrate Integrated Cavity Excitation," *IEEE Antennas and Wireless Propagation Letters*, vol. 17, no. 5, pp. 751–755, Feb. 2018, https://doi.org/10.1109/LAWP.2018.2814051.

[2] Y. Li and K.-M. Luk, "60-GHz Substrate Integrated Waveguide Fed Cavity-Backed Aperture-Coupled Microstrip Patch Antenna Arrays," *IEEE Transactions on Antennas and Propagation*, vol. 63, no. 3, pp. 1075–1085, Mar. 2015, https://doi.org/10.1109/TAP.2015.2390228.

[3] S. Liao, P. Chen, P. Wu, K. M. Shum, and Q. Xue, "Substrate-Integrated Waveguide-Based 60-GHz Resonant Slotted Waveguide Arrays With Wide Impedance Bandwidth and High Gain," *IEEE Transactions on Antennas and Propagation*, vol. 63, no. 7, pp. 2922–2931, Jul. 2015, https://doi.org/10.1109/TAP.2015.2423696.

[4] R. K. Saha, "Spectrum Allocation and Reuse in 5G New Radio on Licensed and Unlicensed Millimeter-Wave Bands in Indoor Environments," *Mobile Information Systems*, vol. 2021, no. 1, 2021, Art. no. 5538820, https://doi.org/10.1155/2021/5538820.

[5] V. Sachan and R. Mishra, "Uplink Sum Rate and Capacity of Hybrid Precoding mmWave Massive MIMO System," *Traitement du Signal*, vol. 36, no. 2, pp. 155–160, Jul. 2019, https://doi.org/10.18280/ts.360205.

[6] S. R. Agilesh, B. T. P. Madhav, A. Gangadhar, and S. S. Chintalapati, "Design of Dual Band Substrate Integrated Waveguide (SIW) Antenna with Modified Slot for Ka-Band Applications," *Engineering, Technology & Applied Science Research*, vol. 14, no. 4, pp. 14923–14928, Aug. 2024, https://doi.org/10.48084/etasr.7620.

[7] T. Djerafi and K. Wu, "60 GHz substrate integrated waveguide crossover structure," in *2009 European Microwave Conference (EuMC)*, Sep. 2009, pp. 1014–1017, https://doi.org/10.23919/EUMC.2009.5296165.

[8] A. Bondarik and D. Sjöberg, "Pattern Reconfigurable Wideband Stacked Microstrip Patch Antenna for 60 GHz Band," *International Journal of Antennas and Propagation*, vol. 2016, no. 1, 2016, Art. no. 5961309, https://doi.org/10.1155/2016/5961309.

[9] S. K. Yong and C.-C. Chong, "An Overview of Multigigabit Wireless through Millimeter Wave Technology: Potentials and Technical Challenges," *EURASIP Journal on Wireless Communications and Networking*, vol. 2007, no. 1, pp. 1–10, Dec. 2006, https://doi.org/10.1155/2007/78907.

[10] Q. Zhu, K. B. Ng, C. H. Chan, and K.-M. Luk, "Substrate-Integrated-Waveguide-Fed Array Antenna Covering 57–71 GHz Band for 5G Applications," *IEEE Transactions on Antennas and Propagation*, vol. 65, no. 12, pp. 6298–6306, Sep. 2017, https://doi.org/10.1109/TAP.2017.2723080.

[11] B. Mishra, R. K. Verma, Y. N, and R. K. Singh, "A review on microstrip patch antenna parameters of different geometry and bandwidth enhancement techniques," *International Journal of Microwave and Wireless Technologies*, vol. 14, no. 5, pp. 652–673, Jun. 2022, https://doi.org/10.1017/S1759078721001148.

[12] M. S. Rabbani and H. Ghafouri-Shiraz, "Improvement of microstrip patch antenna gain and bandwidth at 60 GHz and X bands for wireless applications," *IET Microwaves, Antennas & Propagation*, vol. 10, no. 11, pp. 1167–1173, 2016, https://doi.org/10.1049/iet-map.2015.0672.

[13] R. Addaci and T. Fortaki, "Miniature low profile UWB antenna: New techniques for bandwidth enhancement and radiation pattern stability," *Microwave and Optical Technology Letters*, vol. 58, no. 8, pp. 1808–1813, 2016, https://doi.org/10.1002/mop.29907.

[14] T. Fortaki, S. Benkouda, M. Amir, and A. Benghalia, "Air Gap Tuning Effect on the Resonant Frequency and Half-power Bandwidth of Superconducting Microstrip Patch," *PIERS Online*,

vol. 5, no. 4, pp. 350–354, 2009, https://doi.org/10.2529/PIERS081011143520.

[15] S. Saxena, N. Tewari, A. Kumar, and S. Srivastava, "A Novel Wideband Complementary SIW Backed Edged Spiral Antenna for Radio Telescope Applications," in *2024 IEEE Space, Aerospace and Defence Conference (SPACE)*, Jul. 2024, pp. 952–956, https://doi.org/10.1109/SPACE63117.2024.10668058.

[16] J. Xiao, X. Li, Z. Qi, and H. Zhu, "140-GHz TE_{340} -Mode Substrate Integrated Cavities-Fed Slot Antenna Array in LTCC," *IEEE Access*, vol. 7, pp. 26307–26313, 2019, https://doi.org/10.1109/ACCESS.2019.2900989.

[17] E. Baghernia, R. Movahedinia, and A.-R. Sebak, "Broadband Compact Circularly Polarized Spiral Antenna Array Fed by Printed Gap Waveguide for Millimeter-Wave Applications," *IEEE Access*, vol. 9, pp. 86–95, 2021, https://doi.org/10.1109/ACCESS.2020.3046720.

[18] Y. Liu, D. Isleifson, and L. Shafai, "Gain Enhancement and Cross-Polarization Suppression of Cavity-Backed Antennas Using a Flared Ground Cavity and Iris," *Sensors*, vol. 23, no. 9, Jan. 2023, Art. no. 4389, https://doi.org/10.3390/s23094389.

[19] S. Bedra and T. Fortaki, "Hankel transform domain analysis of covered circular microstrip patch printed on an anisotropic dielectric layer," *Journal of Computational Electronics*, vol. 14, no. 3, pp. 747–753, Sep. 2015, https://doi.org/10.1007/s10825-015-0708-y.